

**Timothy M. Reed,<sup>a</sup> Hidehiko Hirakawa,<sup>a</sup> Minae Mure,<sup>a</sup> Emily E. Scott<sup>b\*</sup> and Julian Limburg<sup>a\*</sup>**<sup>a</sup>Department of Chemistry, The University of Kansas, 1251 Wescoe Hall Drive, Lawrence, KS 66045, USA, and <sup>b</sup>Department of Medicinal Chemistry, 1251 Wescoe Hall Drive, Lawrence, KS 66045, USACorrespondence e-mail: [eescott@ku.edu](mailto:eescott@ku.edu), [jlimburg@ku.edu](mailto:jlimburg@ku.edu)

Received 30 June 2008

Accepted 23 July 2008

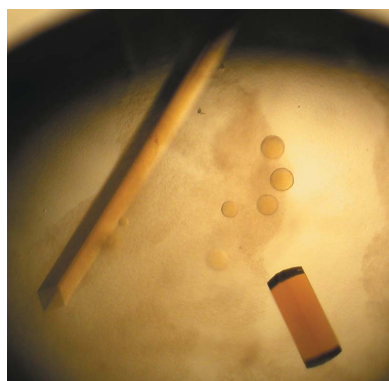
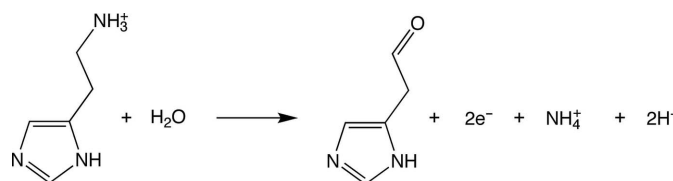
## Expression, purification, crystallization and preliminary X-ray studies of histamine dehydrogenase from *Nocardioides simplex*

Histamine dehydrogenase (HADH) from *Nocardioides simplex* catalyzes the oxidative deamination of histamine to produce imidazole acetaldehyde and an ammonium ion. HADH is functionally related to trimethylamine dehydrogenase (TMADH), but HADH has strict substrate specificity towards histamine. HADH is a homodimer, with each 76 kDa subunit containing two redox cofactors: a [4Fe–4S] cluster and an unusual covalently bound flavin mononucleotide, 6-*S*-cysteinyl-FMN. In order to understand the substrate specificity of HADH, it was sought to determine its structure by X-ray crystallography. This enzyme has been expressed recombinantly in *Escherichia coli* and successfully crystallized in two forms. Diffraction data were collected to 2.7 Å resolution at the SSRL synchrotron with 99.7% completeness. The crystals belonged to the orthorhombic space group  $P2_12_12_1$ , with unit-cell parameters  $a = 101.14$ ,  $b = 107.03$ ,  $c = 153.35$  Å.

### 1. Introduction

Histamine is an essential biogenic amine that is present in prokaryotes and the tissues of animals and plants. In humans, histamine acts as a neurotransmitter, mediates allergic reactions, plays a role in cell proliferation and is important in signaling the release of gastric acid into the stomach (Thurmond *et al.*, 2008). Histamine receptors are the targets of drugs that treat allergies and stomach acidity, but there is very little structural information on the histamine-binding sites of these proteins. Thus, model systems may prove useful for understanding histamine binding (Konkimalla & Chandra, 2003).

Histamine dehydrogenase (HADH) from *Nocardioides simplex* catalyzes the oxidative deamination of histamine to form imidazole acetaldehyde and an ammonium ion (Fig. 1). HADH (Fujieda *et al.*, 2004; Limburg *et al.*, 2005) is related to trimethylamine dehydrogenase (TMADH; EC 1.5.99.7; McIntire, 1990; Steenkamp, Kenney *et al.*, 1978; Steenkamp, McIntire *et al.*, 1978), which contains a 6-*S*-cysteinyl FMN and a [4Fe–4S] cluster. HADH differs from TMADH in its substrate specificity. TMADH acts on short secondary and tertiary amines. In contrast, HADH is selective for the primary amine substrates histamine ( $K_m = 31 \mu\text{M}$ ,  $k_{\text{cat}}/K_m = 2.1 \times 10^5 \text{ M}^{-1} \text{ s}^{-1}$ ), agmatine or decarboxylated arginine ( $K_m = 37 \mu\text{M}$ ,  $k_{\text{cat}}/K_m = 6.0 \times 10^4 \text{ M}^{-1} \text{ s}^{-1}$ ) and putrescine or butane-1,4-diamine ( $K_m = 1280 \mu\text{M}$ ,  $k_{\text{cat}}/K_m = 1500 \text{ M}^{-1} \text{ s}^{-1}$ ) (Limburg *et al.*, 2005). The selectivity for histamine over other biogenic amines suggests that HADH could be used in an amperometric biosensor. Current methods for histamine detection rely on either radioenzymatic or HPLC-based derivatization. The structural determination of HADH, with its unique selectivity for histamine, could prove useful in the design of a histamine biosensor and provide important insights into histamine recognition

© 2008 International Union of Crystallography  
All rights reserved

**Figure 1**  
Histamine-deamination reaction catalyzed by HADH.

by proteins. Furthermore, comparison of the structures of HADH and TMADH may provide insights into the mechanism of this class of enzymes, particularly in regard to the substrate-binding site and the electronic interactions between the two cofactors.

## 2. Materials and methods

### 2.1. Cloning and expression

The *hadh* gene was cloned from genomic DNA of *N. simplex* (ATCC 6946). PCR primers were designed to amplify the 2.1 kbp fragment and incorporate *EcoRI* and *XbaI* sites for subsequent insertion into pUC19. The resulting *hadh* gene was sequenced in the forward and reverse directions and then subcloned between the *NdeI* and *EcoRI* sites of pET21b (Novagen) in order to express the recombinant protein without the C-terminal T7 tag or the N-terminal His tag. The plasmid was transformed into *Escherichia coli* Rosetta 2 (DE3) cells (Novagen). The cells were grown in 1 l Terrific Broth medium with 100 mg l<sup>-1</sup> ampicillin at 310 K and shaking at 225 rev min<sup>-1</sup> to an OD<sub>600</sub> of 0.7. Protein expression was induced with 0.1 mM isopropyl β-D-1-thiogalactopyranoside. The addition of 250 mg l<sup>-1</sup> iron sulfate and 50 mg l<sup>-1</sup> riboflavin was also performed at an OD<sub>600</sub> of 0.7 in order to ensure full incorporation of the iron-sulfur cluster and flavin mononucleotide. The temperature was reduced to 293 K and the cultures were shaken at 225 rev min<sup>-1</sup> overnight. The cells were harvested by centrifugation at 277 K. Selenomethionine-substituted protein was produced using the methionine-auxotrophic *E. coli* strain B834 (DE3) (Novagen; Doublié, 1997).

### 2.2. Purification

Cells (10 g) were resuspended in 20 mM potassium phosphate buffer pH 7.4 containing 0.1 M KCl. Cells were disrupted by ultrasonication and centrifuged at 40 000g for 30 min. The supernatant was loaded onto a 100 ml Toyopearl-DEAE column pre-equilibrated with 20 mM potassium phosphate pH 7.4 containing 0.1 M KCl and proteins were eluted with a 300 ml linear gradient increasing from 0.1 to 0.3 M KCl (20 mM potassium phosphate buffer pH 7.4). Fractions

exhibiting an Abs<sub>444</sub>/Abs<sub>382</sub> ratio of 1.0 or higher were pooled and ammonium sulfate was added to a final concentration of 0.8 M. The protein solution was then loaded onto a 100 ml Toyopearl Butyl-650 column (Tosoh Bioscience) pre-equilibrated with 50 mM potassium phosphate buffer pH 7.4 containing 0.8 M ammonium sulfate. Bound proteins were eluted with a 300 ml gradient decreasing from 0.8 to 0 M ammonium sulfate (50 mM potassium phosphate buffer pH 7.4). Fractions exhibiting an Abs<sub>444</sub>/Abs<sub>382</sub> ratio of 1.2 or higher were pooled and concentrated to 1 ml using an Amicon Ultra centrifugal unit (Millipore). This protein was loaded onto a HiLoad Superdex 200 16/60 sizing column (GE Healthcare) and eluted with 50 mM Tris-HCl pH 7.4 containing 0.15 M KCl. Fractions with an Abs<sub>444</sub>/Abs<sub>382</sub> ratio of 1.38 or higher were concentrated to >20 mg ml<sup>-1</sup>. The purity of HADH was confirmed by SDS-PAGE and the protein concentration was determined using a BCA assay (Thermo Fisher Scientific). The *k*<sub>cat</sub> and *K*<sub>m</sub> for histamine were determined to be 9.8 s<sup>-1</sup> and 24 μM, respectively, using a standard assay (Siddiqui *et al.*, 2000). Selenomethionine-substituted protein was purified as described above and the incorporation of selenomethionine was determined by MALDI-TOF mass spectrometry at KU Analytical Proteomics Laboratory.

### 2.3. Crystallization

Prior to crystallization, the protein was concentrated to 20 mg ml<sup>-1</sup> in 50 mM Tris-HCl buffer pH 7.4 containing 0.15 M KCl. Screening to identify crystallization conditions was performed by the hanging-drop vapor-diffusion method using commercially available sparse-matrix screening kits (Hampton Research and Emerald Biosystems). Equal volumes of protein and reservoir solution (1 μl + 1 μl) were mixed and equilibrated against 750 μl reservoir solution at 293 K.

### 2.4. Data collection and processing

Initial unsubstituted HADH crystals were screened for X-ray diffraction in-house on an R-AXIS IV<sup>++</sup> detector with Cu Kα X-rays generated by a Rigaku RU-H3RHB rotating-anode generator and focused using an Osmic confocal optical system (Rigaku, Japan) at KU Protein Structure Laboratory. A full data set was collected, but initial attempts at molecular replacement using the TMADH structure (PDB code 1djn; Trickey *et al.*, 2000) as a search model were not successful. Subsequently, SeMet-HADH crystals were screened and a complete MAD data set was collected on beamline BL9-2 at the Stanford Synchrotron Radiation Laboratory (SSRL) using the Stanford Automated Mounting (SAM) system (Cohen *et al.*, 2002). Data collection was performed at 100 K using an oscillation angle of 1° per frame over a total of 270° to yield a redundant data set. The diffraction data were processed with *MOSFLM* (Leslie, 2006) and scaled with *SCALA* from the *CCP4* program suite (Collaborative Computational Project, Number 4, 1994).

## 3. Results and discussion

### 3.1. Expression, flavin content, SeMet incorporation and purity

Recombinant unsubstituted HADH was overexpressed in *E. coli* BL21 (DE3) Rosetta strain. The Rosetta strain was used as *hadh* has a high GC content (>85%) with a number of rare codons in the sequence. Expression using this system yielded ~25 mg purified protein per litre of *E. coli* culture. Expression in the methionine-auxotrophic *E. coli* strain B834 (DE3) reduced the yield to ~1/10 of that obtained using Rosetta expression. In order to ensure that the resulting enzyme had a full content of 6-S-cysteinyl-FMN and [4Fe-



**Figure 2**  
Crystals of unsubstituted recombinant HADH grown in 0.1 M HEPES buffer pH 7.4 containing 2.0 M ammonium sulfate, 2% (v/v) PEG 400 and 4% (v/v) glycerol. The crystal to the left is a square rod like those used to collect data, while the crystal on the right is one of the square 'pizza-box' crystals viewed edge-on.

4S], the media were supplemented with the precursors of both cofactors. The percentage of flavination can be determined from the visible spectrum, in which an  $\text{Abs}_{444}/\text{Abs}_{382}$  ratio of 1.4 is consistent with a full complement of 6-*S*-cysteinyl-FMN (Fujieda *et al.*, 2004). Both unsubstituted and SeMet-HADH protein had ratios that were above 1.37. MALDI-TOF mass spectrometry suggested that ten of the 13 methionines were substituted. The recombinant HADH had the same activity towards histamine (both  $k_{\text{cat}}$  and  $k_{\text{cat}}/K_{\text{m}}$ ) as the native enzyme. As estimated by SDS-PAGE, recombinant HADH had the expected molecular weight of 76 kDa and was purified to >99% homogeneity.

### 3.2. Crystallization

Initial yellow crystals grew as both square rods and square 'pizza-box' crystals in 4–7 d in 0.1 M HEPES buffer pH 7.4 containing 2.0 M ammonium sulfate and 2% (v/v) PEG 400 (Fig. 2). The growth of these crystals was then optimized using the same solution, except the protein concentration was varied from 5 to 20 mg ml<sup>-1</sup>. These crystals dissolved rapidly upon opening the sealed wells, but crystallization in the same buffer with the addition of 2–4% (v/v) glycerol obviated this problem and allowed harvesting of diffraction-quality crystals. The crystals used for data collection were square rods that grew to approximately 0.05 × 0.05 × 0.8 mm in size. We determined that a solution consisting of mother liquor with the addition of 25% glycerol was sufficient for cryoprotection of these crystals.

### 3.3. Data collection and preliminary X-ray diffraction analysis

Although we collected a complete three-wavelength MAD data set, structure determination using *SOLVE/RESOLVE* was not immediately successful. However, using only the single-wavelength 0.98 Å data, we were able to determine the structure by molecular replacement using the polypeptide of TMADH from *Methylophilus methylotrophus* (PDB code 1djn; Trickey *et al.*, 2000) as a search model and the program *Phaser* (LLG > 1012; McCoy *et al.*, 2007). The

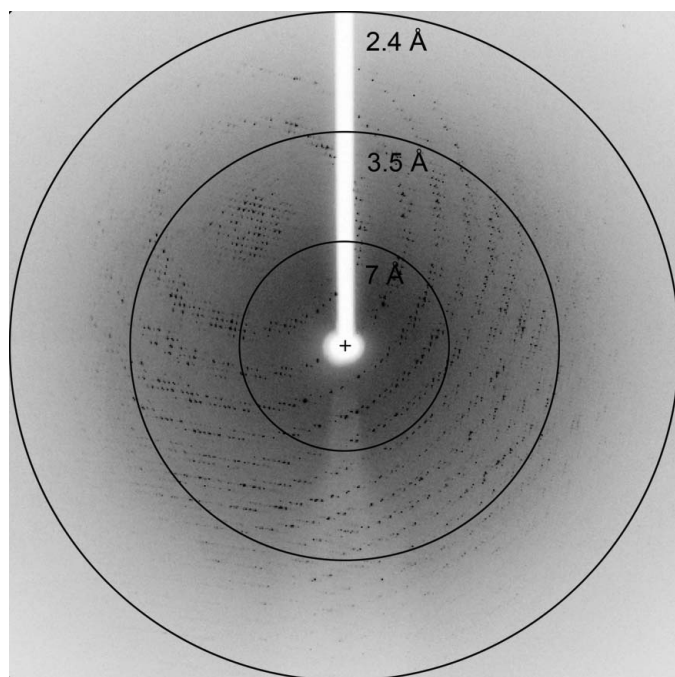


**Figure 3**  
Diffraction pattern of HADH obtained on beamline BL9-2, SSRL. The resolution of this data set was 2.7 Å.

**Table 1**

X-ray data-collection statistics for HADH.

Values in parentheses are for the last resolution shell.

Space group	$P2_12_12_1$
Unit-cell parameters (Å)	$a = 101.14, b = 107.03, c = 153.35$
Resolution (Å)	84.5–2.70 (2.77–2.70)
No. of measurements	451076
No. of unique reflections	46309
Redundancy	9.7 (9.2)
Completeness (%)	99.7 (98.8)
$R_{\text{merge}}$ (%)	16.0 (38.5)
Average $I/\sigma(I)$	16.8 (6.3)

X-ray diffraction data used to solve the HADH structure were collected to a resolution of 2.7 Å (Fig. 3) with 99.7% completeness and an  $R_{\text{merge}}$  of 16% (Table 1). The crystals belong to the orthorhombic space group  $P2_12_12_1$ , with unit-cell parameters  $a = 101.14$ ,  $b = 107.03$ ,  $c = 153.35$  Å. Each asymmetric unit contained two molecules of HADH with a calculated Matthews coefficient  $V_{\text{M}}$  of 2.79 Å<sup>3</sup> Da<sup>-1</sup>, giving an estimated solvent content of 55.96% (Matthews, 1968). Refinement and model building are currently ongoing using *REFMAC* (Murshudov *et al.*, 1997) and *Coot* (Emsley & Cowtan, 2004).

Home-source X-ray data were collected at the Protein Structure Laboratory at The University of Kansas. High-resolution data were collected at the Stanford Synchrotron Radiation Laboratory (SSRL), which provided excellent diffraction facilities and support. The SSRL is operated by the Department of Energy, Office of Basic Energy Sciences. The SSRL Biotechnology Program is supported by the National Institutes of Health, National Center for Research Resources, Biomedical Technology Program and by the Department of Energy, Office of Biological and Environmental Research. This research was supported by NIH GM079446 (JL), NIH 5P20 RR17708 (COBRE Center in Protein Structure and Function) and funds from the University of Kansas Center for Research.

### References

- Cohen, A. E., Ellis, P. J., Miller, M. D., Deacon, A. M. & Phizackerley, R. P. (2002). *J. Appl. Cryst.* **35**, 720–726.
- Collaborative Computational Project, Number 4 (1994). *Acta Cryst.* **D50**, 760–763.
- Doublé, S. (1997). *Methods Enzymol.* **276**, 523–530.
- Emsley, P. & Cowtan, K. (2004). *Acta Cryst.* **D60**, 2126–2132.
- Fujieda, N., Satoh, A., Tsuse, N., Kano, K. & Ikeda, T. (2004). *Biochemistry*, **43**, 10800–10808.
- Konkimalla, V. B. & Chandra, N. (2003). *Biochem. Biophys. Res. Commun.* **309**, 425–431.
- Leslie, A. G. W. (2006). *Acta Cryst.* **D62**, 48–57.
- Limburg, J., Mure, M. & Klinman, J. P. (2005). *Arch. Biochem. Biophys.* **436**, 8–22.
- McCoy, A. J., Grosse-Kunstleve, R. W., Adams, P. D., Winn, M. D., Storoni, L. C. & Read, R. J. (2007). *J. Appl. Cryst.* **40**, 658–674.
- McIntire, W. S. (1990). *Methods Enzymol.* **188**, 250–260.
- Matthews, B. W. (1968). *J. Biol. Chem.* **33**, 491–497.
- Murshudov, G. N., Vagin, A. A. & Dodson, E. J. (1997). *Acta Cryst.* **D53**, 240–255.
- Siddiqui, J. A., Shoeb, S. M., Takayama, S., Shimizu, E. & Yorifuji, T. (2000). *FEMS Microbiol. Lett.* **189**, 183–187.
- Steenkamp, D. J., Kenney, W. C. & Singer, T. P. (1978). *J. Biol. Chem.* **253**, 2812–2817.
- Steenkamp, D. J., McIntire, W. & Kenney, W. C. (1978). *J. Biol. Chem.* **253**, 2818–2824.
- Thurmond, R. L., Gelfand, E. W. & Dunford, P. J. (2008). *Nature Rev. Drug Discov.* **7**, 41–53.
- Trickey, P., Basran, J., Lian, L. Y., Chen, Z. W., Barton, J. D., Sutcliffe, M. J., Scrutton, N. S. & Mathews, F. S. (2000). *Biochemistry*, **39**, 7678–7688.